Kovove Mater. 49 2011 361–367
DOI: 10.4149/km_2011_5_361

Effect of strain rate, volume fraction of particles and temperature on fracture mechanism in Al-Al_4C_3 systems

O. Velgosová[1]*, M. Besterci[2], L. Kováč[2], P. Kulu[3], S.-J. Huang[4]

[1] *Technical University, Faculty of Metallurgy, Department of Non-ferrous Materials and Waste Treatment, Letná 9/A, Košice 042 00, Slovak Republic*
[2] *Institute of Materials Research, Slovak Academy of Sciences, Watsonova 47, Košice 043 53, Slovak Republic*
[3] *Tallin University of Technology, Department of Materials Technology, Ehitajate tee 5, 19086 Tallinn, Estonia*
[4] *National Chung Cheng University, Department of Mechanical Engineering, 168 University Rd., Min-Hsiung, Chia-Yi, Taiwan, R.O.C.*

Received 14 February 2011, received in revised form 21 February 2011, accepted 22 February 2011

Abstract

Changes in the strain and fracture mechanism during tensile testing were investigated in dispersion strengthened Al-Al_4C_3 system. Al materials with volume fraction of 4 and 12 vol.% of Al_4C_3 were tested at temperatures from 293 to 673 K at different strain rates ranging from $\dot{\varepsilon} = 2.5 \times 10^{-5}$ to $10^{-1}\,s^{-1}$. At room temperature, the strain was controlled by dislocation movement and interactions. Work hardening characterized the first part of the strain curve and the second part was characterized by the local strain in the neck. At higher temperatures and strain rates, the number of strain mechanisms was increased by a mechanism attributed to a dynamic recovery process. Fracture mechanism changes depend on temperature and strain rate. At lower temperatures the dispersion strengthened Al-Al_4C_3 system was characterized by transcrystalline fractures. Increase of the test temperature to 523 K and over that, led to intercrystalline fractures for low strain rates $\dot{\varepsilon} = 2.5 \times 10^{-5}\,s^{-1}$.

K e y w o r d s: dispersion strengthened materials, fracture mechanism, SEM analysis

1. Introduction

Dispersion strengthening of the Al matrix is achieved by introducing a small volume fraction of a second-phase into the matrix. The method of powder metallurgy, especially the mechanical alloying, can give a promising structural material production technology. Dispersion strengthened alloys Al-Al_4C_3 prepared by mechanical alloying are characterized by good mechanical properties offering significant weight reduction. They are aimed for use in aircraft, automobile and other industries at room temperature and elevated temperatures [1–3].

The optimized conditions of composite material production by mechanical alloying and the mechanical properties obtained, including plasticity at elevated temperatures, were presented in works [4, 5]. The issue of high temperature stability of this alloy for long time exposition was described in [6]. In works [7, 8], the change of the microstructure after deformation at elevated temperatures was examined and the fracture mechanism of creep was studied. The model of "in-situ" fracture mechanism examination for these materials was described in [9, 10]. Many researchers have been engaged in the kinetics and mechanism of superplastic deformation of various Al alloys, as given in works [11–17].

The aim of this paper is to describe and interpret the fracture mechanism at different strain rates and test temperatures for the Al-Al_4C_3 system with 4 and 12 vol.% of Al_4C_3. Test temperatures ranged from 293 to 673 K and strain rates from $\dot{\varepsilon} = 2.5 \times 10^{-5}$ to $10^{-1}\,s^{-1}$.

2. Experimental material and methods

Mechanical alloying was used for the production of

*Corresponding author: fax: (+42195) 633 70 48; e-mail address: oksana.velgosova@tuke.sk

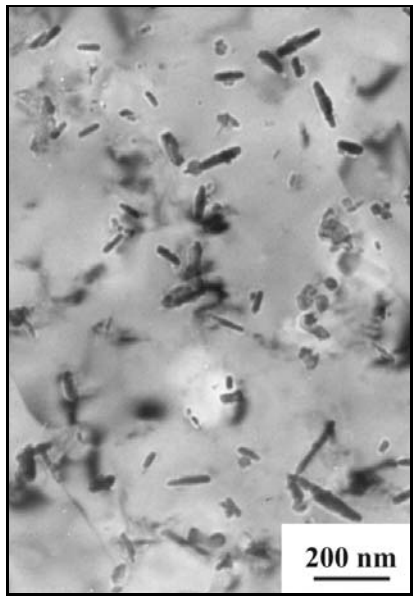

Fig. 1. Size of Al_4C_3 particles on the foil.

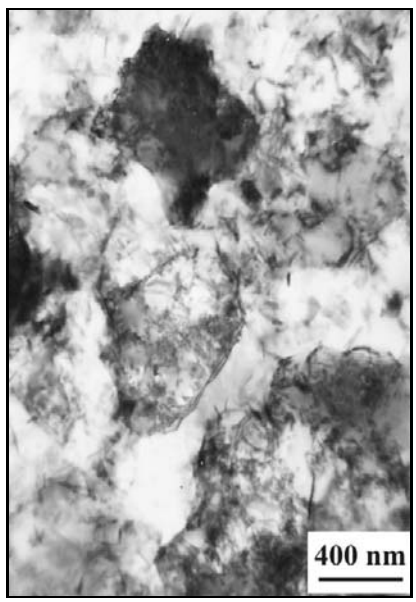

Fig. 2. Grain size of Al matrix on the foil.

Al-Al_4C_3 composites with 4 and 12 vol.% of Al_4C_3.

The Al powder, grain size under 100 μm, was dry milled with KS 2.5 graphite in an attritor for 90 min. The granulate was compacted under the pressure of 600 MPa. The compacts had a cylindrical shape. Subsequent heat treatment at 823 K for 3 h induced a chemical reaction $4Al + 3C \rightarrow Al_4C_3$. The cylinders were then hot extruded at 873 K with 94 % reduction of the cross section. Due to a high affinity of Al to O_2 the system also contains a small amount of Al_2O_3 particles. The volume fraction of Al_2O_3 was lower than 1 vol.%.

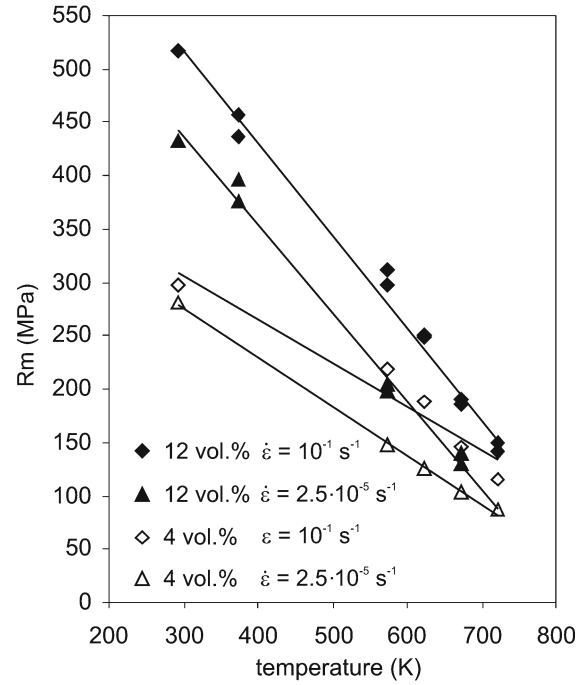

Fig. 3. Influence of temperature, volume fraction and strain rate on tensile strength R_m.

The dispersed particles Al_4C_3 were oriented in rows in the direction of extrusion. The effective sizes of the particles were from 25 to 85 nm, as shown in Fig. 1. There were also larger dispersed particles. Their size was estimated to be from 85 nm to 1 μm, making up about 30 % of the dispersoid amount, observed by SEM. The Al_4C_3 and Al_2O_3 particles were located in the grain boundaries as well as inside in the Al grains. The observed microstructure was fine, even with Al grains less than 1 μm, Fig. 2.

Test pieces, 3 mm in diameter and 15 mm gauge length, were machined for tensile tests. A universal test machine, Tiratest 2300, with a split furnace was used for tensile testing. Digital as well as analogue load on strain dependences were recorded and analysed. The strain rate was calculated from the crosshead speed and the dimensions of the test piece measured before the test. The test pieces were oriented in longitudinal direction, in the direction of extrusion. For the evaluation of strain and fracture mechanisms SEM was used.

3. Results

The results obtained by tensile tests are summarized in Figs. 3 and 4, where the ultimate tensile strength R_m, and the reduction of area Z as a function of temperature and strain rate are shown. The increase of the test temperature caused a decrease of

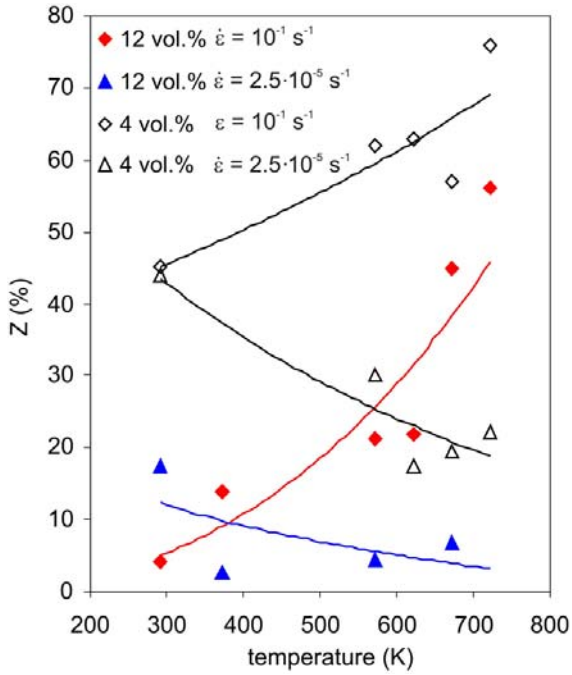

Fig. 4. Influence of temperature, volume fraction and strain rate on reduction of area Z.

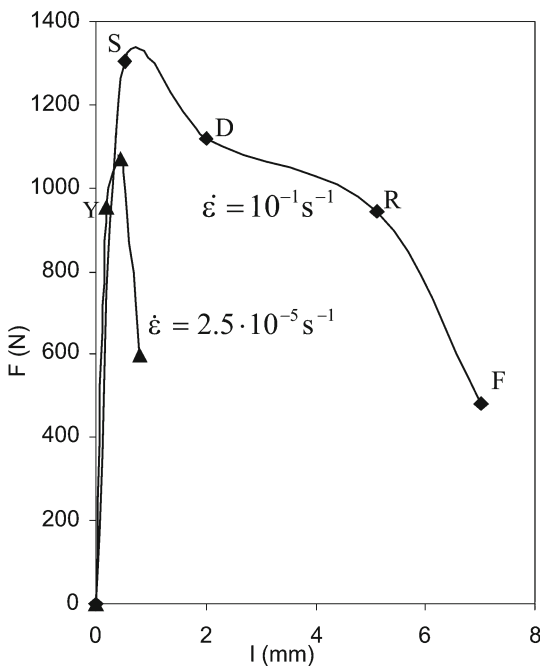

Fig. 5. Characteristics stress-strain curves at 723 K for material with 4 vol. % of Al_4C_3.

strength in all tested materials. The loss of strength was more marked for the material with 12 vol.% of Al_4C_3.

The results with the strain rate of $\dot{\varepsilon} = 10^{-1}\,s^{-1}$ at 673 K for material with 12 vol.% of Al_4C_3 indicated a rapid increase in the value of Z, Fig. 4. However, there was no substantial corresponding change detected in the value of strength.

The rapid increase of area reduction Z with strain rate was evident also for material with 4 vol.% of Al_4C_3 in Fig. 4, though the relative increase was not as high as in the material with 12 vol.% of Al_4C_3. Any increase of plastic properties expressed by reduction of area Z with temperature shows appearance of a new behaviour, something like superplastic behaviour.

The curves in Fig. 5 were obtained at the same test temperature, 723 K. Curves for two different strain rates are marked with labelled points, each label earmarking changes in the nature of the strain process. The shortest elongation was obtained by strain rate $\dot{\varepsilon} = 2.5 \times 10^{-5}\,s^{-1}$. It was $A_5 = 3\,\%$, with reduction of area $Z = 22\,\%$. Even with such a low plasticity there was a clear limit of plastic stability and the following local strain into a neck. The second curve shows the test with strain rate $\dot{\varepsilon} = 10^{-1}\,s^{-1}$. The results were: elongation $A_5 = 34\,\%$, and reduction of area $Z = 75\,\%$. On this curve, the following parts are marked:

– the first part YS is the part of work hardening between the yield point and UTS,

– SD is the start of dynamic weakening,

– DR is the part showing the "plateau", the dynamic recovery, with slow weakening, resulting in uniform, unlocalized plastic deformation in the body of deformed test piece [5],

– RF is the part of the loss of plastic stability, with local deformation into a neck. The measured elongation is the largest. The total value of 34 % is divided to the specified parts by following elongations: YS – 0.8 %, SD – 7.5 %, DR – 15.5 %, RF – 10.2 %.

As known for superplastic strain, the "plateau" should deform at near constant true stress. In our case the weakening was prevailing and the "plateau" was formed at decreasing true stress [6]. This is probably due to three different influences:

a) The mechanical and heat treatment at the production absorbed the part of the deformation capacity for the given grain distribution;

b) At constant crosshead speed there was a decrease of the strain rate during the deformation, with large elongation values it is significant;

c) Voids occurred and developed around dispersed particles and inclusions, damaging the integrity of the material.

At any comparison of mechanical properties with the microstructure of materials, mind, that the strain is accomplished by dislocation gliding. That was the dominant mechanism of plastic deformation. For the material with 4 vol.% of Al_4C_3 at room temperature (293 K) and high strain rate $10^{-1}\,s^{-1}$, the dislocation gliding is in Fig. 6. Higher temperatures cause more dislocation capturing on grain boundaries and on particles. Exceeding the critical value of

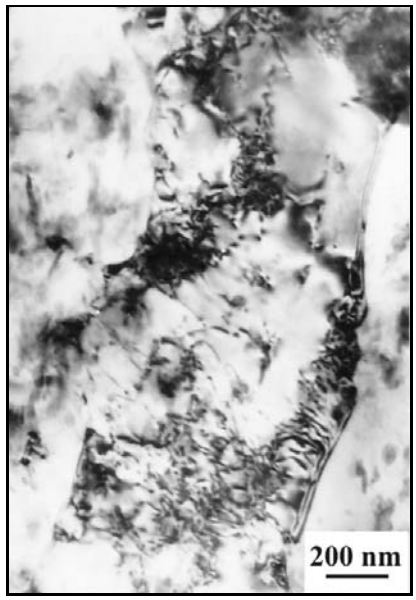

Fig. 6. Dislocation sliding in grain (273 K, $\dot{\varepsilon} = 10^{-1}\,\mathrm{s}^{-1}$).

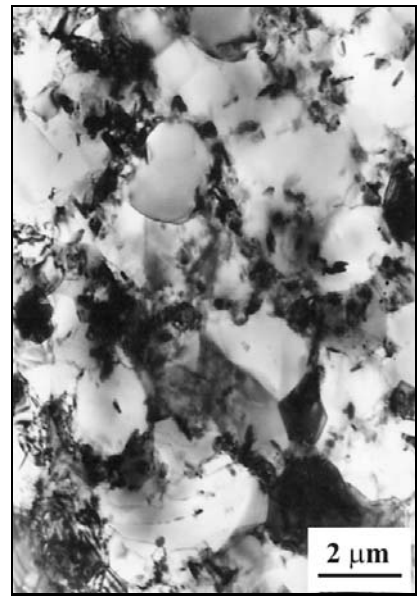

Fig. 8. Polyhedral microstructure obtained by low strain rate and high temperature (723 K, $\dot{\varepsilon} = 2.5 \times 10^{-5}\,\mathrm{s}^{-1}$).

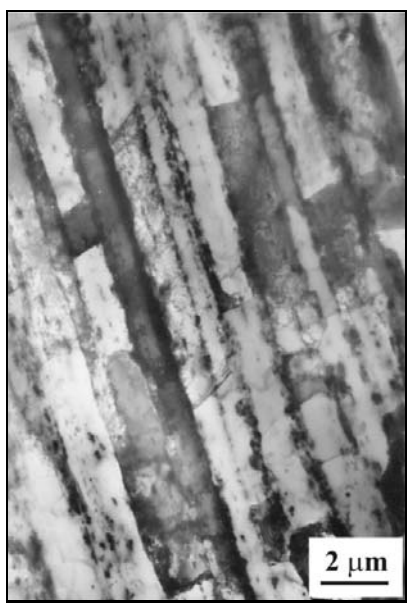

Fig. 7. Microstructure of Al_4C_3 sample in longitudinal direction (723 K, $\dot{\varepsilon} = 10^{-1}\,\mathrm{s}^{-1}$).

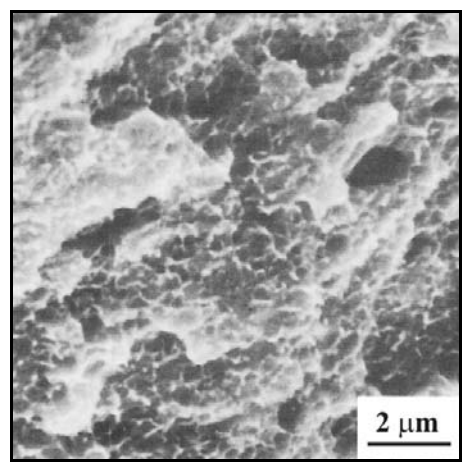

Fig. 9. Transcrystalline fracture surface obtained with strain rate of $\dot{\varepsilon} = 2.5 \times 10^{-5}\,\mathrm{s}^{-1}$ at 293 K for material with 4 vol. % of Al_4C_3.

dislocation density can cause grain boundary gliding. At 723 K and $\dot{\varepsilon} = 10^{-1}\,\mathrm{s}^{-1}$ dynamic polygonization took place. Grains elongated in longitudinal direction, Fig. 7, characterize the microstructure. In the case of low strain rate, polyhedral structure was obtained also at high temperatures, Fig. 8.

The deformation mechanisms of the fracture at different strain rates and temperatures were analysed.

Fracture surface, fractured at room temperature 293 K with low strain rate $\dot{\varepsilon} = 2.5 \times 10^{-5}\,\mathrm{s}^{-1}$ for the material with 4 vol.% of Al_4C_3 is in Fig. 9. The same, for high strain rate $\dot{\varepsilon} = 10^{-1}\,\mathrm{s}^{-1}$, is in Fig. 10. There are no significant differences between them. Both are ductile, at reduction of area $Z = 42\,\%$ and $Z = 45\,\%$, respectively, transcrystalline fractures with dimples. The dimples are shallow with a characteristic dimension of 0.8 μm. Figure 11 shows the fracture surface of the sample loaded with low strain rate $\dot{\varepsilon} = 2.5 \times 10^{-5}\,\mathrm{s}^{-1}$ at 293 K for the material with 12 vol.% of Al_4C_3. The result for the sample with high strain rate of $\dot{\varepsilon} = 10^{-1}\,\mathrm{s}^{-1}$ for the same material is given in Fig. 12. Note, these two samples were ductile and showed transcrystalline fractures with dimples, too.

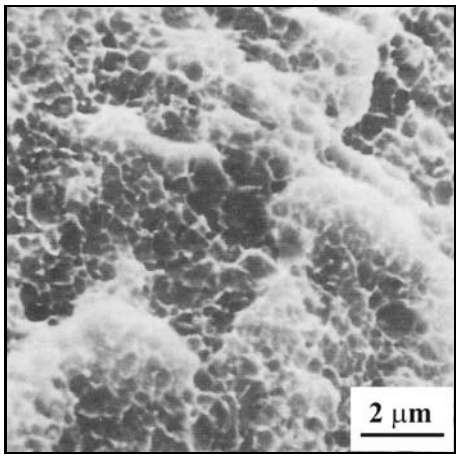

Fig. 10. Transcrystalline fracture surface obtained with strain rate of $\dot{\varepsilon} = 10^{-1}\,\mathrm{s}^{-1}$ at 293 K for material with 4 vol. % of Al_4C_3.

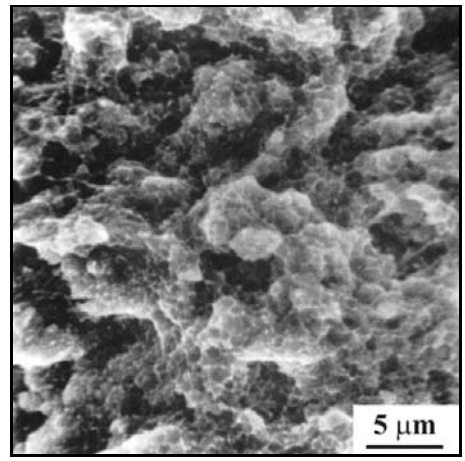

Fig. 12. Transcrystalline fracture surface obtained with strain rate of $\dot{\varepsilon} = 10^{-1}\,\mathrm{s}^{-1}$ at 293 K for material with 12 vol.% of Al_4C_3.

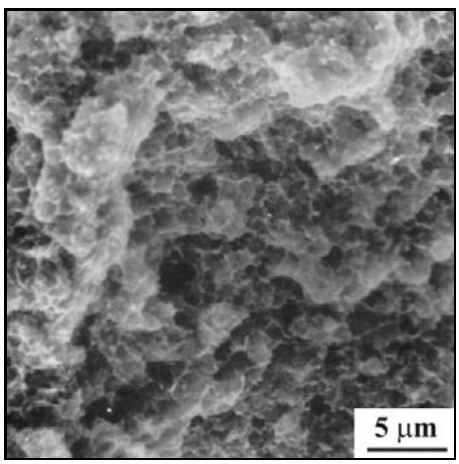

Fig. 11. Transcrystalline fracture surface obtained with strain rate of $\dot{\varepsilon} = 2.5 \times 10^{-5}\,\mathrm{s}^{-1}$ at 293 K for material with 12 vol.% of Al_4C_3.

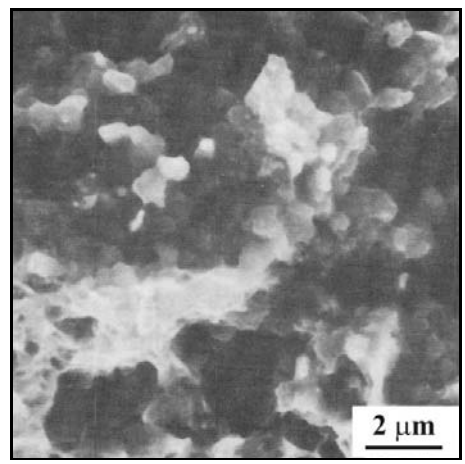

Fig. 13. Intercrystalline fracture surface obtained with strain rate of $\dot{\varepsilon} = 2.5 \times 10^{-5}\,\mathrm{s}^{-1}$ at 723 K for material with 4 vol. % of Al_4C_3.

The dimples were shallow, smaller, with their typical dimension of 0.45 μm.

Fracture surfaces fractured at 573 K and strain rate of $\dot{\varepsilon} = 2.5 \times 10^{-5}\,\mathrm{s}^{-1}$ for material with 12 vol.% of Al_4C_3 showed underdeveloped intercrystalline facets. They were underdeveloped because some ductile fracture takes place at the end of fracture. On the other hand, for high strain rate $\dot{\varepsilon} = 10^{-1}\,\mathrm{s}^{-1}$, the fracture was transcrystalline with dimples. The dimples were deeper and larger than in the case at 293 K. The characteristic dimple diameter was around 0.6 μm.

For material with 4 vol.% of Al_4C_3 fractured at 573 K under strain rate $\dot{\varepsilon} = 2.5 \times 10^{-5}\,\mathrm{s}^{-1}$ the reduction of area was $Z = 16\,\%$. The underdeveloped intercrystalline facets were typical for this fracture. They were underdeveloped because at the end of fracture a faster tearing, ductile fracture finish took place in the form of fine point or line facets with a 100 % reduction of the area. At strain rate of $\dot{\varepsilon} = 10^{-1}\,\mathrm{s}^{-1}$, the fracturing ended with a reduction of area $Z = 64\,\%$. The fracture was transcrystalline with dimples. The dimples were deeper and larger than those at 293 K. The characteristic dimple diameter was around 1.5 μm.

For the high temperature 723 K at low strain rate $\dot{\varepsilon} = 2.5 \times 10^{-5}\,\mathrm{s}^{-1}$ and for material with 4 vol.% of Al_4C_3 the fracture took place at $Z = 22\,\%$. Typical micro facets of the fracture are in Fig. 13. Prevailingly developed intercrystalline facets were present, with dimensions corresponding to the fine grain size, and great angle disorientation. There were small parts of fracture showing crests of ductile facets.

Fracture at the strain rate $\dot{\varepsilon} = 10^{-1}\,\mathrm{s}^{-1}$ ended with a reduction of area $Z = 75\,\%$. The fracture was ductile transcrystalline with developed deep dimples, Fig. 14.

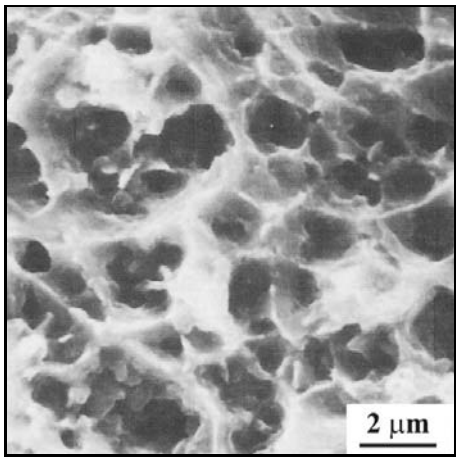

Fig. 14. Transcrystalline fracture surface obtained with strain rate of $\dot{\varepsilon} = 10^{-1}\,\mathrm{s}^{-1}$ at 723 K for material with 4 vol. % of Al_4C_3.

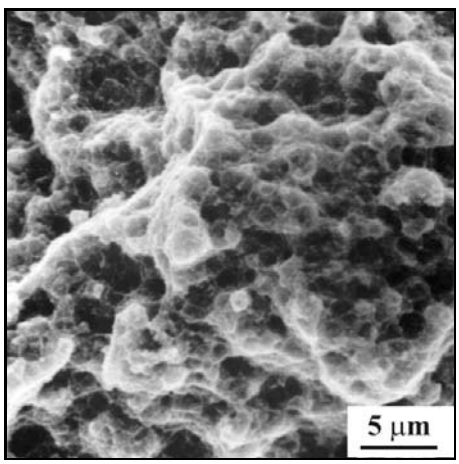

Fig. 15. Intercrystalline fracture surface obtained with strain rate of $\dot{\varepsilon} = 2.5 \times 10^{-5}\,\mathrm{s}^{-1}$ at 673 K for material with 12 vol. % of Al_4C_3.

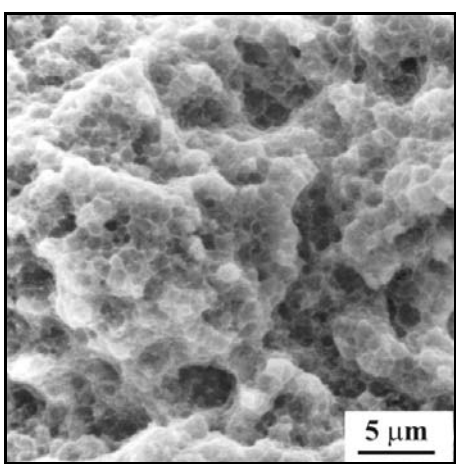

Fig. 16. Transcrystalline fracture surface obtained with strain rate of $\dot{\varepsilon} = 10^{-1}\,\mathrm{s}^{-1}$ at 673 K for material with 12 vol. % of Al_4C_3.

The characteristic dimple dimension was 2 μm.

For low strain rate of $\dot{\varepsilon} = 2.5 \times 10^{-5}\,\mathrm{s}^{-1}$ at 673 K, material with 12 vol.% of Al_4C_3, typical micro facets of the fracture are given in Fig. 15. The reduction of area was only $Z = 8\,\%$. As discussed, developed intercrystalline facets were present, with dimensions corresponding to the fine grain size, and great angle disorientation. There were small parts of fracture showing crests of ductile facets. For the high strain rate of $\dot{\varepsilon} = 10^{-1}\,\mathrm{s}^{-1}$ the fracture ended at the reduction of area $Z = 64\,\%$. The fracture was considered to be ductile transcrystalline with developed deep dimples as shown in Fig. 16. The characteristic dimple dimension was estimated to be 0.65 μm.

4. Discussion

Dislocation gliding in grains was the dominant mechanism of plastic deformation in Al_4C_3 at room temperature (293 K) and high strain rate $10^{-1}\,\mathrm{s}^{-1}$. Higher temperatures cause more dislocation capturing on grain boundaries and on particles. Exceeding the critical value of dislocation density can cause grain boundary gliding.

The analysis of fracture surfaces at 573 K and low strain rate $\dot{\varepsilon} = 2.5 \times 10^{-5}\,\mathrm{s}^{-1}$ showed intercrystalline fractures. We have found damage to grain boundaries formed by interactions of dislocations with dispersed particles in grain boundaries. However, the fine particles in grain boundaries are important for diffusion creep and strength properties of the dispersion strengthened system at high temperatures.

Fractures formed under high strain rates $\dot{\varepsilon} = 10^{-1}\,\mathrm{s}^{-1}$ were transcrystalline. We investigated the microstructure of the broken test pieces by TEM, thin foils and published in [18, 19]. The fracture was caused by voids occurring at the dispersoid-matrix interfaces, first on larger particles, after a great amount of strain. The voids were growing and coalesced into dimples of the transcrystalline fracture. The results confirmed that the deformation process is a combination of:

1. dynamic polygonization as a result of dislocation movement and annihilation;

2. gliding of grain boundaries, which is a part to dislocation creep.

At different strain rates, the contribution of each mechanism is different, and difficult to calculate.

At high strain rates $\dot{\varepsilon} = 10^{-1}\,\mathrm{s}^{-1}$ the dynamic polygonization was remarkable (resulting from a dynamic equilibrium of strengthening and weakening), and gliding of grain boundaries was shown, too. The resulting microstructure after this type of deformation showed recovery and elongated grains [18]. Voids developed in the interfaces dispersoid-matrix. The voids grew into dimples of the transcrystalline fracture.

At low strain rates $2.5 \times 10^{-5}\,\mathrm{s}^{-1}$ dislocation creep

was shown in the microstructure and the grains were uniaxial [19]. The exhausted plasticity of the grain boundaries (first in the triple points) led to intercrystalline fractures.

5. Conclusion

The comparison of the test results and changes in fracture for the Al-Al_4C_3 system at temperatures from 293 to 673 K and strain rates from $\dot{\varepsilon} = 2.5 \times 10^{-5}$ to $\dot{\varepsilon} = 10^{-1}\,s^{-1}$ was summarized:

1. Plastic properties for low strain rate $\dot{\varepsilon} = 2.5 \times 10^{-5}\,s^{-1}$ decrease with increasing temperature. The results are considered relevant to changes in the micromechanism of deformation and fracture. At this strain rate and from temperature 573 K, fracture surfaces show transition from ductile fracture with dimples to intercrystalline fracture, suggesting the exhausted grain boundary plasticity with increasing temperature.

2. Results under high strain rate of $\dot{\varepsilon} = 10^{-1}\,s^{-1}$ at 673 K showed that the first part of the strain characterized by work hardening was very short. At maximum stress, the thermally and mechanically activated dynamic recovery was quite likely to take place, where the strain was uniform all over the body of the test piece. Then there was also quite long part with localized deformation into a neck influenced as well with dynamic recovery. Fracture surfaces remain to be transcrystalline. The higher plastic properties are considered relevant to changes in the micromechanism of deformation and fracture.

Acknowledgements

The work was supported by the Slovak National Grant Agency under the Project VEGA 2/0025/11.

References

[1] JANGG, G.—KORB, G.—KUTNER, F.: Aluminium, *51*, 1975, p. 641.
[2] JANGG, G.—KORB, G.—KUTNER, F.: In: 6. Internationale Leichtmetalltagung. Dusseldorf, Aluminium Verlag 1977, p. 23.
[3] KORB, G.—JANGG, G.—KUTNER, F.: Draht, *5*, 1979, p. 318.
[4] ŠLESÁR, M.—BESTERCI, M.—JANGG, G.—MIŠKOVIČOVÁ, M.—PELIKAN, K.: Werkstofen. Z. Metallkunde, Bd.79(H1), 1988, p. 56.
[5] BESTERCI, M.: Mat. Design, *27*, 2006, p. 416.
[6] ŠLESÁR, M.—JANGG, G.—BESTERCI, M.—ĎURIŠIN, J.—OROLÍNOVÁ, M.: Z. Metallkunde, Bd.80 (H11), 1989, p. 817.
[7] ŠLESÁR, M.—JANGG, G.—ĎURIŠIN, J.—BESTERCI, M.—OROLÍNOVÁ, M.: Mat-Wiss. U. Werkstofftechnik, *23*, 1992, p. 13.
[8] ŠLESÁR, M.—BESTERCI, M.—JANGG, G.: Z. Metallkunde, Bd.83(H3), 1992, p. 183.
[9] BESTERCI, M.—IVAN, J.: J. of Mat. Sci. Letters, *15*, 1996, p. 2071.
[10] BESTERCI, M.—VELGOSOVÁ, O.—IVAN, J.—HVIZDOŠ, J.—KVAČKAJ, T.—KULU, P.: Kovove Mater, 47, 2009, p. 221.
[11] MISHRA, R. S.—MUKHERJEE, A. K.: Mater. Sci. Eng. A, *234–236*, 1997, p. 1023. doi:10.1016/S0921-5093(97)00321-3
[12] BESTERCI, M.—VELGOSOVÁ, O.: Sci and Engineering of Composite Mat., *13*, 2006, p. 283.
[13] BIELER, T. R.—MUKHERJEE, A. K.: Mater. Trans. JIM, *32*, 1991, p. 1149.
[14] NIEH, T. G.—WADSWORTH, J.—IMAI, T.: Scripta Metall., *26*, 1992, p. 703. doi:10.1016/0956-716X(92)90423-C
[15] SAKAI, M.—MUTO, H.: Scripta Mater., *38*, 1998, p. 909. doi:10.1016/S1359-6462(97)00568-X
[16] URENA, A.—GOMÉZ, D. E.—SALAZAR, J. M.—QIUNONES, J.—MARTÍN, J. J.: Scripta Mater., *34*, 1996, p. 617.
[17] BIELER, T. R.—NIEH, T. G.—WADSWORTH, J.—MUKHERJEE, A.: Scripta Metallurgica et Materialia, *22*, 1988, p. 81.
[18] BESTERCI, M.: Dispersion-Strengthened Al System Prepared by Mechanical Alloying. Cambridge, Int. Science Publ. 1999.
[19] BESTERCI, M.—ŠLESÁR, M.—ĎURIŠIN, J.—JANGG, G.—ZBÍRAL, J.: Kovove Mater, *32*, 1994, p. 497.